6A.3 SPRAY-MEDIATED ENTHALPY FLUX TO THE ATMOSPHERE AND SALT FLUX TO THE OCEAN IN HIGH WINDS

Edgar L Andreas*
NorthWest Research Associates, Inc., Lebanon, New Hampshire

1. INTRODUCTION

Evaporating sea spray droplets release water vapor to the near-surface atmosphere. Spray droplets also lose sensible heat to the atmosphere because they originate with the same temperature as the surface ocean but cool rapidly to a temperature lower than the ambient air temperature. Because the sensible heat exchange occurs three orders of magnitude faster than the vapor exchange, spray droplets extract sensible heat from the atmosphere to evaporate and, thus, reclaim some of the sensible heat they have lost. Quantifying the net heating of the atmosphere that is mediated by spray has therefore been illusive.

This net heating is usually termed the enthalpy flux and is the sum of the total air-sea sensible and latent heat fluxes (Businger 1982). I use the adjective "total" here to recognize the possibility that the relevant fluxes comprise contributions from both the usual *interfacial* sensible and latent heat fluxes (directly across the air-sea interface) and the *spray*-mediated fluxes.

Emanuel (1995) explained that, for studying the intensity of tropical cyclones, the enthalpy flux—rather than the individual fluxes of sensible and latent heat—is the "energetically important transfer" from sea to air. He therefore had trouble envisioning how spray could affect storm intensity: That is, throwing a blob of seawater into the air and letting it cool and evaporate there did not seem to transfer any enthalpy from sea to air.

Andreas and Emanuel (2001), however, solved this thermodynamics puzzle. If some of the cooled spray droplets fall back into the sea, they obviously cool the ocean and complete the cycle of enthalpy exchange between sea and air. They termed these *re-entrant* spray droplets and invoked them to demonstrate that sea spray can transfer enthalpy across the air-sea interface. Moreover, Andreas and Emanuel derived a simple parameterization for the enthalpy flux carried by these re-entrant droplets using Andreas and DeCosmo's (1999, 2002) analysis of the HEXOS turbulent heat flux data. (HEXOS was the experiment to study Humidity Exchange over the Sea.)

Here I update Andreas and Emanuel's (2001) parameterization for the spray enthalpy flux by supplementing the HEXOS data with turbulent heat flux data from FASTEX, the Fronts and Atlantic Storm-Tracks Experiment (Joly et al. 1997; Persson et al. 2005). Although the HEXOS and FASTEX sets include wind speeds only up to 20 m s^{-1}, because this parameterization is theoretically based and tuned with data, I have some confidence that it can be extrapolated up to the lower limits of hurricane-strength winds—say to 40 m s^{-1}.

As spray droplets evaporate, they become increasingly saline. By logically following this idea of re-entrant spray droplets, we see that these droplets must also constitute a salt flux to the ocean when they fall back into the sea. To my knowledge, no one has estimated this spray salt flux before or even anticipated it. From the HEXOS and FASTEX data and our previous analysis of the spray fluxes that they imply (Andreas et al. 2008), I here make the first estimate of the spray salt flux.

Even in winds of 15–20 m s^{-1}, that spray salt flux can be 10% of the salt flux resulting from interfacial evaporation. I therefore also develop a fast algorithm for estimating the spray-mediated salt flux to the ocean. In hurricane-strength winds, this spray salt flux should have a significant influence on ocean mixing.

2. RE-ENTRANT SPRAY

Andreas and DeCosmo (2002) and Andreas et al. (2008) modeled the total air-sea latent ($H_{L,T}$) and sensible ($H_{s,T}$) heat fluxes as linear combinations of interfacial and spray contributions:

$$H_{L,T} = H_L + \alpha \overline{Q}_L , \qquad (2.1a)$$

$$H_{s,T} = H_s + \beta \overline{Q}_S + (\gamma - \alpha) \overline{Q}_L . \qquad (2.1b)$$

* *Corresponding author address:* Dr. Edgar L Andreas, NorthWest Research Associates, Inc. (Seattle Division), 25 Eagle Ridge, Lebanon, New Hampshire 03766-1900; e-mail: eandreas@nwra.com.

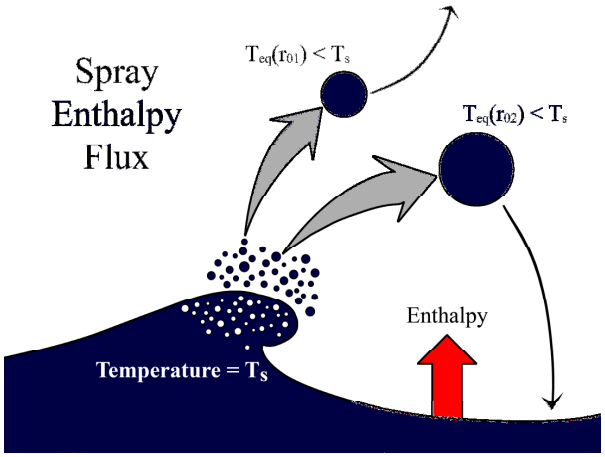

FIG. 1 How sea spray droplets contribute to the flux of enthalpy from sea to air. All droplets cool rapidly from their initial temperature, T_s, to an equilibrium temperature T_{eq} that depends on environmental conditions and droplet radius (denoted r_{01} and r_{02}; $r_{01} < r_{02}$). Smaller droplets remain suspended and do not have an obvious effect on the enthalpy flux; but larger droplets fall back into the sea and clearly cool the ocean, demonstrating that the spray is responsible for a net flux of enthalpy.

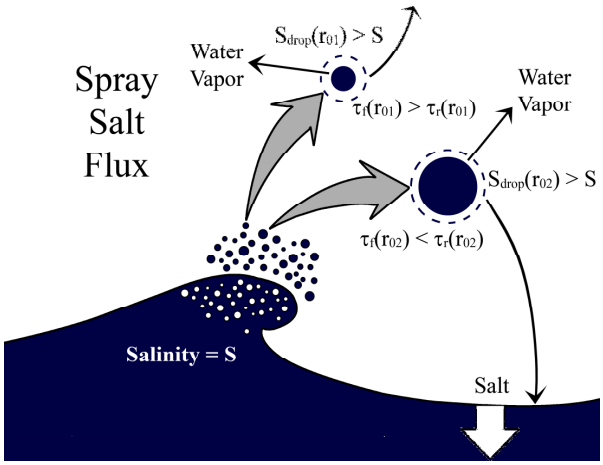

FIG. 2. How sea spray droplets produce a flux of salt to the ocean. All droplets start with ocean salinity S but become more saline through evaporation. Droplets with smaller initial radius (r_{01}) lose water vapor more quickly than larger droplets (radius r_{02}), but the smaller droplets can remain suspended indefinitely. The larger re-entrant droplets, on the other hand, deliver excess salt to the ocean surface. I judge as large droplets those for which their residence time (τ_f) is less than their radius evolution time (τ_r).

Here, H_L and H_s are interfacial latent and sensible heat fluxes estimated with the COARE version 2.6 bulk flux algorithm (Fairall et al. 1996). The $\overline{Q}_L$ and $\overline{Q}_S$ are "nominal" spray fluxes of latent and sensible heat. These come from Andreas's (1989, 1990, 1992) full microphysical spray model and reflect flux contributions integrated over all spray droplets with initial radii, r_0, between 1.6 and 500 μm. The Fairall et al. (1994) spray generation function predicts the rate at which these droplets are formed (Andreas 2002).

I call $\overline{Q}_L$ and $\overline{Q}_S$ "nominal" fluxes because they have proper theoretical dependence on wind speed, humidity, and air and sea surface temperatures but are still uncertain, mainly, because of uncertainties in the spray generation function. The α, β, and γ are small, non-negative coefficients that allowed us to tune this model with the HEXOS and FASTEX data. In (2.1), $\alpha\overline{Q}_L$ is the spray latent heat flux, and $\beta\overline{Q}_S$ is the direct spray sensible heat flux. The $\gamma\overline{Q}_L$ term is a small feedback effect that may be necessary because the evaporating spray cools the near-surface air, thereby increasing the sea-air temperature difference and enhancing H_s above what the COARE algorithm would predict. This term, thus, is an indirect spray effect.

For their analysis, Andreas et al. (2008) interpreted $H_{L,T}$ and $H_{s,T}$ as the HEXOS and FASTEX fluxes obtained by eddy-covariance measurements at heights of 8–20 m above the sea surface. In modeling applications, once (2.1) are tuned with data, their predictions of $H_{L,T}$ and $H_{s,T}$ could serve as the lower flux boundary conditions for an atmospheric model or the upper boundary conditions for an ocean model.

The total enthalpy flux is just the sum of (2.1a) and (2.1b):

$$Q_{en,T} = H_{L,T} + H_{s,T} = H_L + H_s + \beta\overline{Q}_S + \gamma\overline{Q}_L \,. \quad (2.2)$$

Notice here, the main spray latent heat flux term, $\alpha\overline{Q}_L$, drops out with this summation, as it should. The only effect of spray latent heat on the total enthalpy flux is thus through the $\gamma\overline{Q}_L$ term, the presumably small feedback term. Meanwhile, the sensible heat flux associated with re-entrant spray, the $\beta\overline{Q}_S$ term, is the primary mechanism by which spray affects enthalpy transfer.

Figures 1 and 2 show my conceptual picture

of how spray droplets affect the air-sea fluxes of enthalpy and salt.

Figure 1 depicts spray droplets forming with initial temperature T_s, the sea surface temperature. All droplets cool within seconds, however, to an equilibrium temperature, T_{eq}, that is lower than the air temperature and depends on environmental conditions and the droplet radius at formation, r_0 (Andreas 1990, 1995, 1996). The droplets also lose water by evaporation (not depicted in Fig. 1). Because this is a slower process than the temperature evolution and therefore occurs while the droplets are at T_{eq}, the latent heat for that evaporation must reflect a conversion from sensible heat in the near-surface air [i.e., the $-\alpha\overline{Q}_L$ terms in (2.1b)]. As a result, whether spray droplets ultimately heat or cool the air is not obvious at first.

In fact, if droplets were to evaporate entirely (as freshwater droplets could) or were to stay suspended indefinitely, their net effect would be hard to deduce. But the larger droplets fall back into the sea. Because $T_{eq} < T_s$, these clearly cool the ocean. This thought experiment therefore demonstrates that sea spray transfers enthalpy from sea to air.

Andreas (1990, 1992) introduced three droplet time scales to help us decide what "large" droplets are. I have been using as an estimate of a droplet's residence time, τ_f, the ratio of the significant wave height ($H_{1/3}$) to the droplet's fall speed (u_f):

$$\tau_f = \frac{H_{1/3}}{2u_f}. \qquad (2.3)$$

The temperature evolution time, τ_T, is the e-folding time for the droplet's cooling:

$$\frac{T(t) - T_{eq}}{T_s - T_{eq}} = \exp(-t/\tau_T), \qquad (2.4)$$

where T is the droplet temperature and t is the time since formation. The radius evolution time, τ_r, is the corresponding e-folding time for the droplet's evaporation to an equilibrium radius, r_{eq}:

$$\frac{r(t) - r_{eq}}{r_0 - r_{eq}} = \exp(-t/\tau_r), \qquad (2.5)$$

where r is the droplet's instantaneous radius.

Andreas (1992), Andreas and DeCosmo (1999), and Andreas et al. (1995) show plots that compare τ_r, τ_T, and τ_r. All of these time scales depend on initial droplet radius, air temperature and humidity, and surface salinity. τ_f also depends on the wind speed because I use Andreas and Wang's (2007) formulation to estimate $H_{1/3}$ in the absence of measurements of $H_{1/3}$. For all droplets, $\tau_T \ll \tau_r$.

When the discussion is about enthalpy transfer, large droplets are those that fall back into the sea locally: They have τ_f values of, say 10 s or less. Droplets with r_0 greater than 20–120 μm, depending on wind speed, are therefore large droplets in this context (e.g., Andreas and DeCosmo 1999).

Figure 2 sketches how spray droplets affect the salt flux to the ocean. Here, droplets start with the same salinity S as the ocean surface. Because of evaporation, though, droplet salinity increases from S. Smaller droplets, which evaporate more quickly, are saltier than large droplets. But many of these smaller droplets remain suspended indefinitely; only the larger re-entrant spray droplets deliver excess salt to the ocean. Later, I will assume that large droplets in this context are ones for which $\tau_f < \tau_r$. That is, their atmospheric residence time is less than their radius evolution time scale. Depending on wind speed, r_0 is greater than 20–50 μm for droplets that contribute to the salt flux [see Andreas and DeCosmo's (1999) plot of τ_f and τ_r].

3. DATA

Andreas et al. (2008) described the HEXOS and FASTEX data sets. Briefly, the HEXOS data came directly from tabulations in DeCosmo's (1991) thesis. Andreas and DeCosmo (2002) described some preprocessing that we had to do to obtain the required variables. The HEXOS set includes eddy-covariance measurements of the friction velocity (u_*) and the total sensible ($H_{s,T}$) and latent ($H_{L,T}$) heat fluxes on the Meetpost Noordwijk platform in the North Sea. Smith et al. (1992), Katsaros et al. (1994), and DeCosmo et al. (1996) provided thorough descriptions of the instrument and the measurements. The HEXOS set contains 175 runs with turbulent fluxes and associated mean meteorological quantities collected in 10-m winds up to 18.3 m s^{-1}.

The FASTEX set also includes eddy-covariance measurements of the three turbulent fluxes (u_*, $H_{s,T}$, and $H_{L,T}$) and associated mean meteorological quantities. These came from instruments placed on the bow mast of the *R/V Knorr* while the ship made a winter transect across

the North Atlantic from England to Nova Scotia (Persson et al. 2005). The FASTEX set includes 322 hourly flux measurements in winds up to 22 m s^{-1}.

Both HEXOS and FASTEX sets also include measurements of the significant wave height, $H_{1/3}$, for use in (2.3). Andreas et al. (2008) explain other details of how we manipulated the HEXOS and FASTEX data to compute values of H_s, H_L, $\overline{Q}_S$, and $\overline{Q}_L$ in (2.1) and (2.2).

4. SPRAY ENTHALPY FLUX

The analysis by Andreas et al. (2008) yielded the values for H_s, H_L, $\overline{Q}_S$, and $\overline{Q}_L$ that I use here. I estimate H_s and H_L from the COARE version 2.6 bulk flux algorithm (Fairall et al. 1996), with some slight changes as described by Andreas et al. Fairall et al (2003) updated the COARE algorithm to version 3.0. I prefer version 2.6 for my application here, however, because its calculations of temperature (z_T) and humidity (z_Q) roughness lengths, which are required for computing H_s and H_L, are based on the surface renewal theory of Liu et al. (1979). Because this algorithm is theoretically based and proven accurate (e.g., Fairall et al. 1996; Grant and Hignett 1998; Chang and Grossman 1999) for treating the interfacial sensible and latent heat fluxes in winds up to 10 m s^{-1}, I have some faith that it will still be accurate when extrapolated to higher wind speeds.

In the COARE version 3.0 algorithm, on the other hand, Fairall et al. (2003) determined z_T and z_Q by fitting data collected in winds up to 20 m s^{-1}. My previous work has concluded that spray contributions to the heat fluxes become significant when winds reach 10–15 m s^{-1}. Hence, I believe that this newer COARE algorithm mixes spray and interfacial fluxes in its estimates of z_T and z_Q and, therefore, is not useful for separating spray and interfacial contributions in the HEXOS and FASTEX data sets.

Andreas et al. (2008) computed $\overline{Q}_S$ and $\overline{Q}_L$ from Andreas's (1989, 1990, 1992) microphysical spray model. A key component of this is the spray generation function, which predicts the rate at which droplets of radius r_0 are produced at the sea surface. We used the Fairall et al. (1994) form for this function [equations in Andreas (2002)].

The first issue in evaluating the total air-sea enthalpy flux, (2.2), is to decide whether spray makes any difference. That is, do we really need to augment the COARE version 2.6 estimates of the interfacial fluxes H_s and H_L with spray contributions, as (2.2) implies (cf. Andreas and DeCosmo 2002; Andreas et al. 2008)? Figures 3 and 4 answer this question.

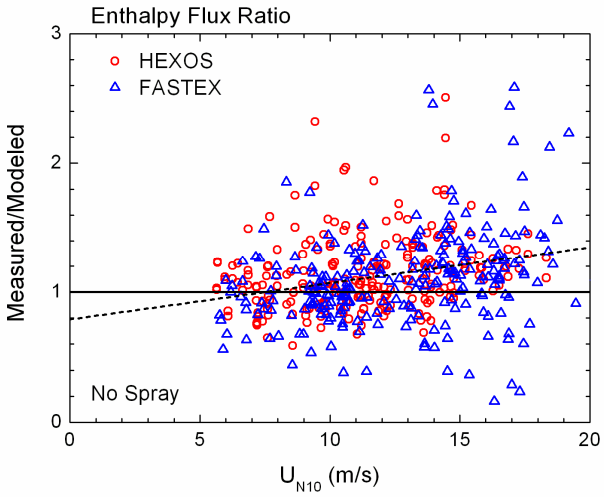

FIG. 3. The ratio of HEXOS and FASTEX measurements of the total enthalpy flux ($Q_{en,T} = H_{L,T} + H_{s,T}$) to the enthalpy flux modeled as just the interfacial contribution (i.e., no spray effect; $Q_{en,int} = H_L + H_s$). The abscissa is the neutral-stability wind speed at a reference height of 10 m, which is tabulated in both the HEXOS and FASTEX sets. The cloud of points averages 1.1249, and the correlation coefficient is 0.2609.

Figure 3 shows the ratio of the measured total enthalpy flux,

$$Q_{en,T} = H_{L,T} + H_{s,T}, \qquad (4.1)$$

to the modeled interfacial enthalpy flux,

$$Q_{en,int} = H_L + H_s. \qquad (4.2)$$

In these, $H_{L,T}$ and $H_{s,T}$ are the HEXOS and FASTEX flux measurements, and H_L and H_s are estimates of the interfacial fluxes from the COARE version 2.6 algorithm.

If the COARE algorithm were sufficient for predicting the total enthalpy flux, the ratios $Q_{en,T}/Q_{en,int}$ in Fig. 3 would not depend on wind speed, and the average of all values would be one. That is, the COARE algorithm alone would explain both the magnitude and the wind speed dependence of the HEXOS-FASTEX set. Figure 3 demonstrates, however, that a strictly interfacial flux algorithm is inadequate on both counts. Using statistics described in Andreas et al. (2008), I

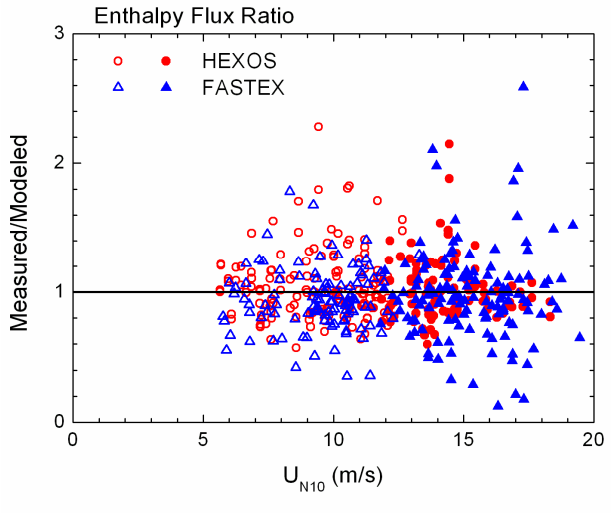

FIG. 4. As in Fig. 3, except here I add spray effects to the interfacial fluxes (H_L and H_s) in (2.2) by setting $\beta = 18.08$ and $\gamma = 0$. The points in the figure now average 0.9991, and the correlation coefficient of the enthalpy flux ratio with U_{N10} is 0.0000. Filled symbols are cases for which the spray enthalpy flux, $\beta\overline{Q}_S$, is at least 10% of the interfacial enthalpy flux, $H_L + H_s$.

confirm that the average of the points in Fig. 3, 1.1249, is significantly above one and that the correlation coefficient, 0.2609, is significantly different from zero. In other words, the model is biased low and does not explain the wind dependence of the data.

Both of these tests suggest enhanced enthalpy transfer with increasing wind speed. To me, this is a signature of spray effects. Hence, the next issue is whether the candidate expression for the total enthalpy flux, (2.2), which combines interfacial and spray contributions, can explain this enhanced transfer. Figure 4 demonstrates that it can.

Figure 4 is like Fig. 3—the ratio of measured-to-modeled enthalpy fluxes. But in Fig. 4, I account for spray effects by adjusting β and γ in (2.2). Actually, I produced Fig. 4 with γ set to zero. That is, I explain the magnitude and the wind speed dependence of the HEXOS and FASTEX enthalpy fluxes by just finding the β value for which the cloud of points in Fig. 4 averages one and the correlation coefficient is essentially zero. With $\beta = 18.08$ (and $\gamma = 0$), (2.2) meets both conditions. The average of the ratios in Fig. 4 is 0.9991, and the correlation coefficient is 0.0000.

I see no a priori guarantee that the flux algorithm (2.2), with one adjustable spray parameter, must center the cloud of points in Fig. 4 around one and simultaneously remove the wind speed dependence in the data. The fact that my simple theoretically based algorithm can do both gives it credence.

The filled symbols in Fig. 4 demonstrate that spray processes begin to have a significant effect on the total air-sea enthalpy flux at modest wind speeds. For these filled circles, the modeled spray enthalpy flux ($\beta\overline{Q}_S$) is at least 10% of the modeled interfacial enthalpy flux ($H_L + H_s$). Most of the points for U_{N10} greater than 12 m s^{-1} are filled.

In effect, this analysis separates the total measured enthalpy flux into interfacial and spray contributions:

$$Q_{en,int} = H_L + H_S , \qquad (4.3a)$$

$$Q_{en,sp} = \beta\overline{Q}_S . \qquad (4.3b)$$

Here, $Q_{en,int}$ comes fairly quickly from the COARE algorithm. But finding $Q_{en,sp}$ involves integrating over the contributions for all spray droplets with radii (r_0) between 1.6 and 500 µm and is, therefore, too computationally intensive for any large-scale modeling.

We had noticed, however, that droplets with r_0 values near 100 µm dominate the spray sensible heat flux (Andreas and Emanuel 2001; Perrie et al. 2005; Andreas et al. 2008). Hence, as a fast spray enthalpy flux algorithm, I follow Andreas and Emanuel's (2001) lead and assume that these 100-µm droplets are reliable indicators of the spray enthalpy flux. The fast flux parameterization thus becomes

$$Q_{en,sp} = \beta\overline{Q}_S = \rho_w c_w \left(T_s - T_{eq,100}\right) V_{en}(u_*) . \quad (4.4)$$

Here ρ_w (1000 kg m^{-3}) is the water density; c_w (4000 J kg^{-1}), the specific heat of seawater (e.g., Andreas 2005b); and $T_{eq,100}$, the equilibrium temperature of droplets that start with radius $r_0 = 100$ µm.

Also in (4.4), $V_{en}(u_*)$ is a wind function that depends only on the friction velocity, u_*. I evaluate it from my partitioning of the HEXOS and FASTEX data as

$$V_{en}(u_*) = \frac{Q_{en,sp}}{\rho_w c_w \left(T_s - T_{eq,100}\right)} . \qquad (4.5)$$

Figure 5 shows the plot of these data. Here, u_* is

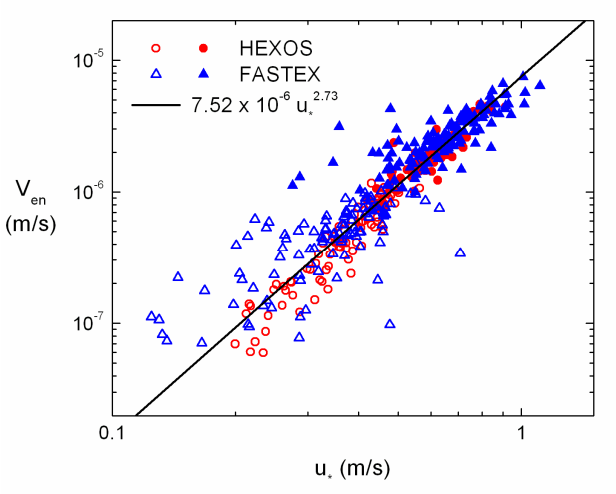

FIG. 5. The wind function V_{en} in (4.4) as evaluated from the HEXOS and FASTEX enthalpy flux data according to (4.5). The correlation coefficient is 0.917. The line is (4.6), where u_* is the measured friction velocity. Filled symbols denote cases for which the modeled spray enthalpy flux ($\beta\overline{Q}_S$) is at least 10% of the modeled interfacial enthalpy flux ($H_L + H_s$).

the measured friction velocity, and I evaluated $T_{eq,100}$ from my fast spray microphysical algorithms (Andreas 2005a).

The data in Fig. 5 cluster well around the power-law relation

$$V_{en}(u_*) = 7.52\times10^{-6}\,u_*^{2.73}, \qquad (4.6)$$

which gives V_{en} in m s^{-1} when u_* is in m s^{-1}. The evidence in Fig. 5 that (4.4) and (4.6) represent the spray enthalpy flux fairly well justifies the validity of such a simple parameterization.

Equation (4.6) gives somewhat smaller values of V_{en} than the corresponding relation in Andreas and Emanuel [2001; their (8)], which was based on just the HEXOS data. The wind speed dependence in (4.6) (i.e., $u_*^{2.73}$), however, is almost as strong as Andreas and Emanuel found (i.e., u_*^3) and reiterates why spray processes become increasingly important in storm winds.

The filled symbols in Fig. 5 again denote cases for which the modeled spray enthalpy flux is at least 10% of the corresponding interfacial flux. Most symbols for which $u_* > 0.5$ m s^{-1} are filled and therefore indicate a significant spray contribution to the total enthalpy flux.

5. SPRAY SALT FLUX

Using my full microphysical model, I estimate the spray latent heat flux in two parts (cf. Andreas 1992; Andreas and DeCosmo 2002; Andreas et al. 1995, 2008):

For $\tau_f \le \tau_r$,

$$Q_L(r_0) = \rho_w L_v \left\{1 - \left[\frac{r(\tau_f)}{r_0}\right]^3\right\}\left(\frac{4\pi r_0^3}{3}\frac{dF}{dr_0}\right); \qquad (5.1a)$$

for $\tau_f > \tau_r$,

$$Q_L(r_0) = \rho_w L_v \left[1 - \left(\frac{r_{eq}}{r_0}\right)^3\right]\left(\frac{4\pi r_0^3}{3}\frac{dF}{dr_0}\right). \qquad (5.1b)$$

Here, Q_L is the flux contribution from all droplets at each radius r_0, L_v is the latent heat of vaporization, and $r(\tau_f)$ is the droplet radius when the droplet falls back into the sea. For these calculations, I obtained $r(\tau_f)$ by using the microphysical model to track the evolution of droplet radius for each r_0.

The dF/dr_0 in (5.1) is the spray generation function—the rate at which droplets of initial radius r_0 are formed. It has units of number of droplets produced per square meter of sea surface, per second, per micrometer increment in droplet radius. Again, for dF/dr_0, I used the same function that Fairall et al. (1994) used.

The nominal spray latent heat flux comes from integrating (5.1) over all droplets that make significant contributions:

$$\overline{Q}_L = \int_{1.6}^{500} Q_L(r_0)\,dr_0\,. \qquad (5.2)$$

Here the limits of integration are in micrometers.

As explained earlier, only droplets that experience some evaporation and then fall back into the sea can accomplish a salt flux to the ocean. Equation (5.1a) represents most of these although there is an uncertain range around $\tau_f = \tau_r$ for which it is unclear whether a droplet remains suspended or is re-entrant. Based on our current level of understanding, (5.1a) is therefore my best guess as to how to estimate the spray salt flux.

If the interfacial latent heat flux is H_L, the associated salt flux is

$$F_{salt} = \frac{sH_L}{L_v(1-s)}\,. \qquad (5.3)$$

Here, s is the fractional salinity. That is, if the salinity S is 34 psu, s = 0.034. My sign convention is that, if H_L is positive, the vapor flux is upward—from ocean to atmosphere. Consequently, F_{salt} is positive when the salt flux is into the ocean surface.

In analogy with (5.3), (5.1a) gives the approximate spray salt flux to the ocean that is contributed by droplets of radius r_0 as

$$Q_{salt}(r_0) = \frac{\rho_w s}{1-s}\left\{1-\left[\frac{r(\tau_f)}{r_0}\right]^3\right\}\left(\frac{4\pi r_0^3}{3}\frac{dF}{dr_0}\right) \quad (5.4)$$

for $\tau_f \le \tau_r$. In turn, the nominal spray salt flux is

$$\overline{Q}_{salt} = \int_{r_{min}}^{500} Q_{salt}(r_0)\,dr_0\,, \quad (5.5)$$

where r_{min} is the value of r_0 for which $\tau_f(r_0) = \tau_r(r_0)$ and is a function of wind speed and other environmental conditions.

In tuning the nominal spray latent heat flux, $\overline{Q}_L$, to produce an accurate estimate of the spray latent heat flux, $\alpha\overline{Q}_L$, Andreas et al. (2008) had the luxury of using data to evaluate α to be 1.50. Without such data for tuning the spray salt flux, I can only assume that the same tuning coefficient applies to the salt flux. That is, I estimate the spray salt flux as

$$Q_{salt,sp} = \alpha\overline{Q}_{salt}\,, \quad (5.6)$$

where α is still 1.50.

Figure 6 shows calculations of the interfacial and spray salt fluxes based on the HEXOS and FASTEX data. As earlier, H_L in (5.3) comes from my adaptation of the COARE version 2.6 algorithm (see Andreas et al. 2008), and $\overline{Q}_{salt}$ in (5.6) comes from my full microphysical model. The interfacial salt flux is generally somewhat larger than $10^{-6}\,kg\,m^{-2}\,s^{-1}$ and increases slightly as U_{N10} increases from 5 to 20 m s^{-1}. The spray salt flux, in contrast, is less than $10^{-8}\,kg\,m^{-2}\,s^{-1}$ in a 5-m s^{-1} wind but increases dramatically to almost $10^{-6}\,kg\,m^{-2}\,s^{-1}$ for a 20-m s^{-1} wind.

Figure 6 implies that, for wind speeds above the range for which I have data, the spray salt flux will likely become comparable to or even exceed the interfacial salt flux. Such a flux to the ocean is in no current models but will affect ocean stratification and, thus, ocean mixing in storm

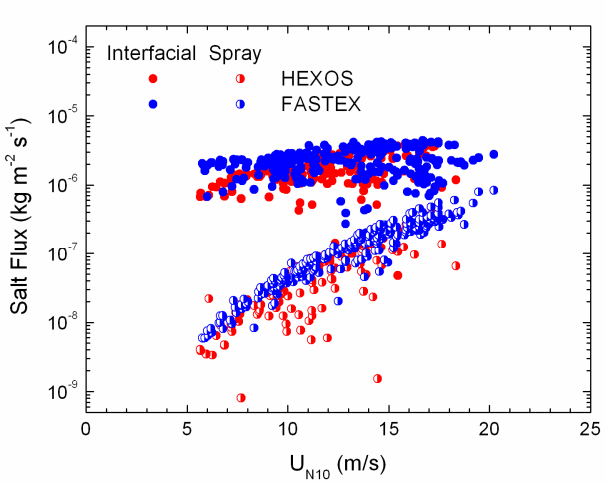

FIG. 6. The interfacial and spray salt fluxes are computed from the HEXOS and FASTEX data using (5.3) and (5.6), respectively, and are plotted against the neutral-stability wind speed at a height of 10 m.

winds. Adding a spray salt flux in coupled ocean-atmosphere models may therefore help explain changes in the intensity of tropical cyclones.

But my method for computing (5.6) here is too computationally intense. As with computing the spray enthalpy flux, we need a faster algorithm. When faced with a similar requirement, Andreas et al. (2008) postulated that spray droplets that start with a radius r_0 of 50 μm are good indicators of the spray latent heat flux. Because $\tau_f \le \tau_r$ for these droplets and because the peak in the $Q_{salt}(r_0)$ spectrum is near 50 μm, I postulate that they are also key indicators of the spray salt flux. My fast flux algorithm thus becomes

$$Q_{salt,sp} = \frac{\rho_w s}{1-s}\left\{1-\left[\frac{r(\tau_{f,50})}{50\,\mu m}\right]^3\right\}V_{salt}(u_*)\,, \quad (5.7)$$

where the α in (5.6) is incorporated into V_{salt}. In (5.7), $\tau_{f,50}$ is the residence time of droplets that start with a radius of 50 μm; hence, the 50 μm also takes the place of r_0 in (5.4). Furthermore, I estimate $r(\tau_{f,50})$ from (2.5) in the form

$$r(\tau_{f,50}) = r_{eq,50} + (50\,\mu m - r_{eq,50})\exp(\tau_{f,50}/\tau_{r,50})\,, \quad (5.8)$$

where all radii are in micrometers. Andreas's (2005a) fast microphysical algorithm—rather than the full microphysical model—provides $r_{eq,50}$ and

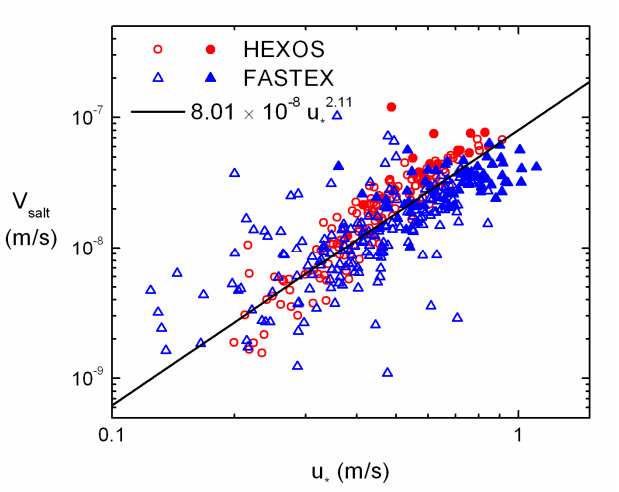

FIG. 7. The wind function V_{salt} in (5.7) as evaluated from the HEXOS and FASTEX salt flux data according to (5.9). The correlation coefficient is 0.765. The line is (5.10), where u_* is the measured friction velocity. Filled symbols denote cases for which the spray salt flux [$\alpha\overline{Q}_{salt}$ from (5.6)] is at least 10% of the interfacial salt flux [F_{salt} from (5.3)].

$\tau_{r,50}$, respectively, the equilibrium radius of droplets that started at 50 μm and the time scale for that evolution.

The remaining unknown in (5.7) is the wind function $V_{salt}(u_*)$. The spray salt flux data plotted in Fig. 6 provide this as

$$V_{salt}(u_*) = \frac{Q_{salt,sp}}{\frac{\rho_w s}{1-s}\left\{1-\left[\frac{r(\tau_{f,50})}{50\,\mu m}\right]^3\right\}} \quad . \qquad (5.9)$$

Figure 7 shows this function.

The best fitting line in Fig. 7 is

$$V_{salt}(u_*) = 8.01\times10^{-8}\,u_*^{2.11} \quad , \qquad (5.10$$

which give V_{salt} in m s^{-1} for u_* in m s^{-1}. The data in Fig. 7 scatter about this line more than the data in Fig. 5 scatter about their fitting line. But the facts that the data cluster around this power-law relation and have a correlation coefficient of 0.765 argue for the usefulness of (5.7) as a good place to start in parameterizing the spray salt flux in models.

6. CONCLUSIONS

Tropical cyclones extract enthalpy from the ocean as their source of power. Traditionally, that enthalpy transfer is parameterized as an exchange across the air-sea interface. But theory and observations suggest that that interfacial enthalpy exchange is not large enough to explain storm intensity. Here, however, I have shown that spray-mediated enthalpy transfer augments the interfacial transfer: This spray enthalpy flux may be a missing piece required for explaining storm intensity.

I have demonstrated the importance of the spray enthalpy flux by using eddy-covariance measurements of the sensible and latent heat fluxes from HEXOS and FASTEX. The sum of these fluxes is the total air-sea enthalpy flux. A state-of-the-art flux algorithm that treats just the interfacial transfer cannot, however, reproduce this total enthalpy flux. Only when I add a theoretically based model for the spray-mediated enthalpy flux to the interfacial flux algorithm can I explain both the magnitude and the wind speed dependence of the HEXOS and FASTEX data.

These calculations essentially separated the HEXOS and FASTEX flux measurements into interfacial and spray enthalpy fluxes. From the spray fluxes, I then developed a fast algorithm for predicting the spray enthalpy flux in large-scale models. That algorithm is based on the premise that droplets with an initial radius of 100 μm dominate the spray enthalpy flux and introduces a wind function V_{en} that goes as $u_*^{2.73}$, where u_* is the friction velocity. This strong dependence on u_* emphasizes why spray processes are important in storm winds.

Building on Andreas and Emanuel's (2001) idea of re-entrant spray, I realized that spray droplets constitute a salt flux to the ocean when they re-enter it. Again using my full spray microphysical model and the HEXOS and FASTEX data, I made the first estimate of this spray salt flux. It starts lower but increases more rapidly with wind speed than the salt flux resulting from interfacial evaporation and likely will dominate the salt flux to the ocean in hurricane-force winds.

From the spray salt flux that my modeling deduced from the HEXOS and FASTEX data, I developed a fast algorithm for estimating the spray salt flux for use in large-scale models. This algorithm presumes that droplets that start with radius 50 μm are good indicators of the spray salt flux. The wind function V_{salt}, which is key to this

algorithm, goes as $u_*^{2.11}$; thus, as with enthalpy, the spray salt flux becomes increasingly important in storm winds.

7. ACKNOWLEDGMENTS

I thank Ola Persson, Jeff Hare, Chris Fairall, and Bill Otto for providing the FASTEX data and Emily B. Andreas for help with the graphics. The Office of Naval Research supported this work with grant N000140810411.

8. REFERENCES

Andreas, E. L, 1989: Thermal and size evolution of sea spray droplets. CRREL Rep. 89-11, U.S. Army Cold Regions Research and Engineering Laboratory, Hanover, NH, 37 pp. [NTIS: ADA210484.]

_____, 1990: Time constants for the evolution of sea spray droplets. *Tellus*, **42B**, 481–497.

_____, 1992: Sea spray and the turbulent air-sea heat fluxes. *J. Geophys. Res.*, **97**, 11,429–11,441.

_____, 1995: The temperature of evaporating sea spray droplets. *J. Atmos. Sci.*, **52**, 852–862.

_____, 1996: Reply. *J. Atmos. Sci.*, **53,** 1642–1645.

_____, 2002: A review of the sea spray generation function for the open ocean. *Atmosphere-Ocean Interactions*, Vol. 1, W. Perrie, Ed., WIT Press, 1–46.

_____, 2005a: Approximation formulas for the microphysical properties of saline droplets. *Atmos. Res.*, **75**, 323–345.

_____, 2005b: Handbook of physical constants and functions for use in atmospheric boundary layer studies. *ERDC/CRREL Monograph M-05-1*, U.S. Army Cold Regions Research and Engineering Laboratory, Hanover, NH, 42 pp.

_____, and J. DeCosmo, 1999: Sea spray production and influence on air-sea heat and moisture fluxes over the open ocean. *Air-Sea Exchange: Physics, Chemistry and Dynamics*, G. L. Geernaert, Ed., Kluwer, 327–362.

_____, and _____, 2002: The signature of sea spray in the HEXOS turbulent heat flux data. *Bound.-Layer Meteor.*, **103**, 303–333.

_____, and K. A. Emanuel, 2001: Effects of sea spray on tropical cyclone intensity. *J. Atmos. Sci.*, **58**, 3741–3751.

_____, and S. Wang, 2007: Predicting significant wave height off the northeast coast of the United States. *Ocean Eng.*, **34**, 1328–1335.

_____, J. B. Edson, E. C. Monahan, M. P. Rouault, and S. D. Smith, 1995: The spray contribution to net evaporation from the sea: A review of recent progress. *Bound.-Layer Meteor.*, **72**, 3–52.

_____, P. O. G. Persson, and J. E. Hare, 2008: A bulk turbulent air-sea flux algorithm for high-wind, spray conditions. *J. Phys. Oceanogr.*, **38,** 1581–1596.

Businger, J. A., 1982: The fluxes of specific enthalpy, sensible heat and latent heat near the Earth's surface. *J. Atmos. Sci.*, **39**, 1889–1892.

Chang, H.-R., and R. L. Grossman, 1999: Evaluation of bulk surface flux algorithms for light wind conditions using data from the Coupled Ocean-Atmosphere Response Experiment (COARE). *Quart. J. Roy. Meteor. Soc.*, **125**, 1551–1588.

DeCosmo, J., 1991: Air-sea exchange of momentum, heat and water vapor over whitecap sea states. Ph.D. dissertation, University of Washington, 212 pp.

_____, K. B. Katsaros, S. D. Smith, R. J. Anderson, W. A. Oost, K. Bumke, and H. Chadwick, 1996: Air-sea exchange of water vapor and sensible heat: The Humidity Exchange over the Sea (HEXOS) results. *J. Geophys. Res.*, **101**, 12,001–12,016.

Emanuel, K. A., 1995: Sensitivity of tropical cyclones to surface exchange coefficients and a revised steady-state model incorporating eye dynamics. *J. Atmos. Sci.,* **52**, 3969–3976.

Fairall, C. W., J. D. Kepert, and G. J. Holland, 1994: The effect of sea spray on surface energy transports over the ocean. *Global Atmos. Ocean Syst.*, **2**, 121–142.

_____, E. F. Bradley, D. P. Rogers, J. B. Edson, and G. S. Young, 1996: Bulk parameterization of air-sea fluxes for Tropical Ocean-Global Atmosphere Coupled-Ocean Atmosphere Response Experiment. *J. Geophys. Res.*, **101**, 3747–3764.

_____, _____, J. E. Hare, A. A. Grachev, and J. B. Edson, 2003: Bulk parameterization of air-sea fluxes: Updates and verification for the COARE algorithm. *J. Climate*, **16**, 571–591.

Grant, A. L. M., and P. Hignett, 1998: Aircraft observations of the surface energy balance in TOGA-COARE. *Quart. J. Roy. Meteor. Soc.*, **124**, 101–122.

Joly, A., and 19 others, 1997: The Fronts and Atlantic Storm-Track Experiment (FASTEX): Scientific objectives and experimental design. *Bull. Amer. Meteor. Soc.*, **78**, 1917–1940.

Katsaros, K. B., J. DeCosmo, R. J. Lind, R. J. Anderson, S. D. Smith, R. Krann, W. Oost, K. Uhlig, P. G. Mestayer, S. E. Larsen, M. H. Smith, and G. de Leeuw, 1994: Measurements of humidity and temperature in the marine environment during the HEXOS Main Experiment. *J. Atmos. Oceanic Technol.*, **11**, 964–981.

Liu, W. T., K. B. Katsaros, and J. A. Businger, 1979: Bulk parameterization of air-sea exchanges of heat and water vapor including the molecular constraints at the interface. *J. Atmos. Sci.*, **36**, 1722–1735.

Perrie, W., E. L Andreas, W. Zhang, W. Li, J. Gyakum, and R. McTaggart-Cowan, 2005: Sea spray impacts on intensifying midlatitude cyclones. *J. Atmos. Sci.*, **62**, 1867–1883.

Persson, P. O. G., J. E. Hare, C. W. Fairall, and W. D. Otto, 2005: Air-sea interaction processes in warm and cold sectors of extratropical cyclonic storms observed during FASTEX. *Quart. J. Roy. Meteor. Soc.*, **131**, 877–912.

Smith, S. D., R. J. Anderson, W. A. Oost, C. Krann, N. Maat, J. DeCosmo, K. B. Katsaros, K. L. Davidson, K. Bumke, L. Hasse, and H. Chadwick, 1992: Sea surface wind stress and drag coefficients: The HEXOS results. *Bound.-Layer Meteor.*, **60**, 109–142.